

Published in *Prog. Theor. Phys.* **94**(1995), pp 1019-1038.

Microscopic  $\alpha$ -Cluster Model for  $^{12}\text{C}$  and  $^{16}\text{O}$  Based on  
Antisymmetrized Molecular Dynamics

— *Consistent Understanding of the Binding Energies of*  
 $^{12}\text{C}$  *and*  $^{16}\text{O}$  —

Naoyuki ITAGAKI, Akira OHNISHI and Kiyoshi KATŌ

*Department of Physics, Hokkaido University, Sapporo 060*

**Abstract**

In many previous calculations within microscopic models, the binding energy difference between  $^{12}\text{C}$  and  $^{16}\text{O}$  nuclei has been too large compared with the experimental data, and these nuclei have not been able to describe reasonably by the same effective interaction simultaneously. In this paper, we apply the  $N\alpha$ -cluster model so as to clarify what is the most essential problem in description of  $^{12}\text{C}$  and  $^{16}\text{O}$ , by using a very large functional space and various effective interactions. This procedure is carried out by combining frame works of the constraint cooling method introduced in Antisymmetrized Molecular Dynamics (AMD) and generator coordinate method (GCM). The resultant energy levels of  $^{16}\text{O}$  show that the various effective interactions give the second  $0^+$  state of  $^{16}\text{O}$  just around the  $^{12}\text{C}+\alpha$  threshold energy which agrees with the picture of the Ikeda diagram. However, even if we use some density dependent interactions, the binding energy difference between  $^{12}\text{C}$  and  $^{16}\text{O}$  can not be remarkably improved.

# 1 Introduction

The  $\alpha$ -cluster models have signally succeeded in understanding many properties of light  $4N$  nuclei.<sup>1)</sup> As a typical example, we can cite many studies of the  $3\alpha$ -cluster model for  $^{12}\text{C}$ , which have been carried out by using formulations of Resonating Group Method (RGM),<sup>2)</sup> Generator Coordinate Method (GCM),<sup>3)</sup> and Orthogonal Condition Model (OCM).<sup>4)</sup> These calculations have shown the  $3\alpha$ -cluster model to reproduce successfully the energy levels of many excited states including the second  $0^+$  state which is hardly explained by a simple shell model.<sup>5)</sup> In the context of recent developments of nuclear-astronomy and unstable nuclear physics, it is very interesting to apply reliable cluster models to the related topics. For example, it is needed to prepare precise wave functions based on the cluster model in order to understand recent experimental data such as the astrophysical  $S$ -factor of the  $\alpha+^{12}\text{C}\rightarrow^{16}\text{O}+\gamma$  reaction and the  $\beta$  decay partial widths of  $^{16}\text{N}$ .<sup>6, 7)</sup>

In heavier  $4N$  nuclei such as  $^{16}\text{O}$ ,  $^{20}\text{Ne}$  and  $^{24}\text{Mg}$ , the cluster models have also been applied. In their studies of low-lying states of those nuclei, many calculations have been done on the basis of assumptions of two- or three-cluster configurations (a core+ $\alpha$  or a core+ $2\alpha$  configuration); a  $^{12}\text{C}+\alpha$  model for  $^{16}\text{O}$ ,<sup>8, 9, 10)</sup>  $^{16}\text{O}+\alpha$ ,<sup>11)</sup> and  $^{12}\text{C}+2\alpha$  models for  $^{20}\text{Ne}$ ,<sup>12)</sup> and a  $^{16}\text{O}+2\alpha$  model for  $^{24}\text{Mg}$ .<sup>13)</sup> On the other hand, as was shown in the so-called Ikeda diagram,<sup>14)</sup> the cluster degrees of freedom in the assumed core nuclei activate with increasing excitation energies, and various kinds of multi-cluster configurations are expected to appear around the corresponding threshold energies. For example, according to the Ikeda diagram, it is expected that the  $^{24}\text{Mg}$  nucleus has  $^{20}\text{Ne}+\alpha$ ,  $^{12}\text{C}+^{12}\text{C}$ ,  $^{16}\text{O}+\alpha+\alpha$ ,  $^{12}\text{C}+3\alpha$  and finally  $6\alpha$ -cluster or molecular configurations in excited states as the excitation energy increases. Recently, a new molecular resonance has been observed by Wuosmaa *et al.*<sup>15)</sup> in the excitation function of the inelastic reaction  $^{12}\text{C}(^{12}\text{C}, ^{12}\text{C}(0_2^+))^{12}\text{C}(0_2^+)$  at  $E_x=56.4$  MeV. As one candidate to explain such a resonance state in  $^{24}\text{Mg}$ , a  $6\alpha$ -chain state has been discussed.<sup>16)</sup> To investigate such a structure change problem and multi-cluster structures in highly-excited energies, it is necessary to extend the framework of cluster models. As far as light  $4N$  nuclei, it is desired to establish a  $N\alpha$ -cluster model, in which all the  $\alpha$ -cluster degrees of freedom are dynamically treated.

As one of serious problems in the microscopic cluster model, it has been pointed out that the binding energies of  $^{12}\text{C}$  and  $^{16}\text{O}$  cannot be reproduced consistently by using a common nuclear interaction. For  $^{16}\text{O}$ , Suzuki<sup>9, 10)</sup> has explained most of low excited levels by the frame work of the semi-microscopic OCM. In this model, however, the  $^{12}\text{C}$  internal wave functions have been fixed in the simple  $(\lambda, \mu)=(0, 4)$   $SU_3$  model configuration which includes the ground rotational band states ( $0^+$ ,  $2^+$  and  $4^+$ ). Furthermore, the experimental values have been used for the binding and excitation energies of  $^{12}\text{C}$ , and the strength of the folding potential between  $^{12}\text{C}$  and  $\alpha$  has been adjusted to fit the binding energy of  $^{16}\text{O}$ . On the other hand, Horiuchi<sup>8)</sup> has suggested that the microscopic  $^{12}\text{C}+\alpha$  model without any auxiliary parameters for the binding and excitation energies of the  $^{12}\text{C}$ -cluster cannot reproduce the binding energy of  $^{16}\text{O}$  and also the excitation energy of the  $0_2^+$  state at 6.05 MeV. This problem essentially comes from the difficulty that the binding energies of  $^{12}\text{C}$  and  $^{16}\text{O}$  are not consistently reproduced. And this difficulty is very serious in studying not only  $^{16}\text{O}$  but also heavier  $4N$  nuclei. Because  $^{12}\text{C}$  and  $^{16}\text{O}$  nuclei are milestones in the cluster model, and these nuclei in addition to  $\alpha$  are important building blocks in various kind of cluster configurations as was shown, for example, about the structure change in the  $^{24}\text{Mg}$  nucleus.

We here investigate a fully microscopic  $N\alpha$ -cluster model focusing our main attention on the following problems:

- 1) How to solve a many-body problem with many degrees of freedom.
- 2) What kind of interactions between nucleons should be used which gives consistent understanding of various nuclei ?

To overcome the first problem, we employ Antisymmetrized Molecular Dynamics (AMD) developed by Horiuchi *et al.*<sup>17)~21)</sup> In AMD, the cooling method is used to obtain the energy minimum in the large dimensional parameter space. We apply the cooling method of AMD to the Bloch-Brink wave function<sup>22)</sup> of the  $N\alpha$  system and seek for the energy minimum of an  $N\alpha$  configuration with several constraints. By carrying out this process, we can get many different cooled intrinsic states, and by superposing these states as GCM basis states, we can obtain more reliable wave functions in a very large functional space describing the ground state and lower excited states. This AMD+GCM will be examined by applying to the  $3\alpha$  system and by comparing the results with the previous calculations. Its conclusion will be shown to be that our method is a very powerful way to treat many degrees of freedom and to construct reliable wave functions of the ground state and also excited states.

The second problem of effective interactions is a more physical one. As was mentioned above, it has been a long standing problem to reproduce  $^{12}\text{C}$  and  $^{16}\text{O}$  binding energies by using a common effective interaction with the same parameter. However, before criticizing the effective interaction, we should carefully investigate the model space used in calculations. Many cluster models of  $^{16}\text{O}$  have assumed a  $^{12}\text{C}+\alpha$  configuration and also a specific configuration such as a simple  $SU_3$  shell model wave function for the  $^{12}\text{C}$ -cluster. In order to discuss the binding energy problem of  $^{12}\text{C}$  and  $^{16}\text{O}$  on a common base, we must take away those assumptions. For this purpose, we apply a  $4\alpha$  model to  $^{16}\text{O}$  and solve the  $4\alpha$  dynamics by using the method developed here. We do not have any assumption except that the wave functions are limited to those of the  $\alpha$ -cluster model. Since the  $^{12}\text{C}$  is well described by the  $3\alpha$  dynamics, we will naturally obtain  $^{12}\text{C}+\alpha$  solutions of the  $4\alpha$  system if such configurations are realized in the ground or excited states of  $^{16}\text{O}$ .

As will be shown, the binding energies of  $^{12}\text{C}$  and  $^{16}\text{O}$  cannot reasonably be reproduced under various kinds of effective  $NN$  interactions, even though a very wide model space is taken into account for  $^{16}\text{O}$ . We investigate this problem by introducing a three-body interaction. Fukatsu and one (K.Katō) of the present authors<sup>23)</sup> have shown that the binding energies of  $^{12}\text{C}$  and  $^{16}\text{O}$  are reproduced within the  $4\alpha$  OCM by introducing an effective  $3\alpha$  potential. However, their calculation was not a fully microscopic but a semi-microscopic. Recently, Tohsaki<sup>24)</sup> has proposed an effective three-nucleon interaction with finite ranges, and discussed that in addition to the binding energies of some  $4N$  nuclei, the saturation point of nuclear matter is reproduced with this interaction. However, he assumed the  $SU_3$   $(\lambda, \mu)=(0,4)$  configuration for  $^{12}\text{C}$  and the closed-shell configuration for  $^{16}\text{O}$  in his calculation. It is very interesting to examine this three-body interaction on improvement of both binding energies of  $^{12}\text{C}$  and  $^{16}\text{O}$  in a wide model space without any specific geometric configuration.

In the present paper, we extensively investigate the binding energy problem of  $^{12}\text{C}$  and  $^{16}\text{O}$  based on the microscopic  $3\alpha$  and  $4\alpha$  models by trying to use some kinds of effective two- or three-nucleon interactions. Furthermore, we discuss reliability of the models through analyses of excited level structures of these nuclei. The results of the  $4\alpha$  model strongly suggest the realization of the  $^{12}\text{C}+\alpha$  structure in the  $0_2^+$  state of  $^{16}\text{O}$ , which is obtained around the  $^{12}\text{C}+\alpha$  threshold energy. On the other hand, the binding energies of  $^{12}\text{C}$  and  $^{16}\text{O}$  are not enough reproduced even if we introduced the three-body interaction, though the

Tohsaki force gives a little improvement in calculated binding energies.

From this study, we discuss which is the essential difficulty in the binding energy problem of  $^{12}\text{C}$  and  $^{16}\text{O}$ , namely an under-binding problem of  $^{12}\text{C}$  or an over-binding problem of  $^{16}\text{O}$ . Our final conclusion is that the former will be more essential. Its reasons and possibility of the improvement in the under-binding of  $^{12}\text{C}$  will be discussed.

This paper is organized as follows, in §2, we explain our model especially about AMD constraint cooling method and the way to construct GCM wave functions. In §3, we show our results of  $^{12}\text{C}$  and  $^{16}\text{O}$ . In the first and second subsection, we check a reliability of our model by comparing our  $^{12}\text{C}$  results with other calculations. Next we carry out  $4\alpha$  GCM for  $^{16}\text{O}$  with the effective interaction Volkov No.2<sup>25)</sup> and discuss resultant energy levels in the third subsection. For the consistent understanding with  $^{12}\text{C}$ , finally we also present the result of some density dependent interactions in the fourth subsection. In §4, we give discussion on the usefulness of our AMD+GCM framework and the binding energy problem of  $^{12}\text{C}$  and  $^{16}\text{O}$ . In §5 summary and conclusion are presented.

## 2 Method

In this section we explain our wave function and the way to construct the GCM basis states. We use a local Gaussian form for single particle wave functions where generator coordinates are extended to complex values describing the position and momentum of each  $\alpha$ -cluster. However, it is not easy in the case of a many- $\alpha$  system how to choose GCM basis states. In the traditional  $3\alpha$ -cluster GCM carried out by Uegaki *et al.*<sup>3)</sup>, they have superposed many GCM basis states which are given by various types of  $3\alpha$  geometric configurations. Such a way becomes very difficult in four- or more-body system because of their large number of basis states. In return we use a variational principle to search for suitable phase space parameters so as to minimize the energy of the nucleus under some constraints. This method is proposed in the frame work of AMD<sup>17)</sup> and called the frictional cooling method.<sup>18)~21)</sup> We expect that cooled states searched for in a large variational space well describe the ground state and lower excited states.

### 2.1 Wave function

We have adopted the Bloch-Brink wave function<sup>22)</sup> for an  $N\alpha$  system, which is given by the Slater determinant of Gaussian wave packets.<sup>17, 18)</sup> Assuming the [4]-symmetry for the spin and iso-spin part of single nucleon in an  $\alpha$ -cluster, we express a single nucleon wave function as follows;

$$\phi_i^\alpha(\vec{r}; \vec{Z}_i) = \exp\{-\nu(\vec{r} - \vec{Z}_i/\sqrt{\nu})^2 + \vec{Z}_i^2/2\}\chi_\alpha, \quad (1)$$

$$\chi_\alpha = \{\text{p } \uparrow, \text{ p } \downarrow, \text{ n } \uparrow, \text{ n } \downarrow\}, \quad i = 1 \sim N.$$

In the spatial part,  $\nu$  means the size parameter and the complex parameter

$$\vec{Z}_i = \sqrt{\nu}(\vec{D}_i + i\vec{K}_i/2\nu\hbar) \quad (2)$$

represents phase space coordinates which consists of the real spatial part  $\vec{D}_i$  and the momentum part  $\vec{K}_i$ . The total wave function of the  $N\alpha$ -cluster system is given by the totally antisymmetrized product of these single nucleon wave functions  $\{\phi_i^\alpha(\vec{r}_i^\alpha; \vec{Z}_i)\}$ ;

$$\Phi(\{\vec{Z}_i; \vec{r}_i^\alpha\}) = \mathcal{A} \prod_{i=1}^N \prod_{\alpha=1}^4 \phi_i^\alpha(\vec{r}_i^\alpha; \vec{Z}_i). \quad (3)$$

### 2.2 Cooling method and the angular momentum projection

By treating  $\{\vec{Z}_i\}$  as a set of variational parameters, we search the energy minimum configuration within the wave function given in Eq.(3). This procedure is performed by assuming the variational parameter  $\{\vec{Z}_i\}$  to be a function of a single real parameter  $\beta$ , and by solving the following equations (cooling equation);<sup>18)~21)</sup>

$$\frac{d\vec{Z}_i}{d\beta} = -\frac{\partial\mathcal{H}}{\partial\vec{Z}_i^*}, \quad \frac{d\vec{Z}_i^*}{d\beta} = -\frac{\partial\mathcal{H}}{\partial\vec{Z}_i}, \quad (4)$$

where  $\mathcal{H}$  is the expectation value of the Hamiltonian;

$$\mathcal{H} = \frac{\langle \Phi(\{\vec{Z}_i; \vec{r}_i^\alpha\}) | \hat{H} | \Phi(\{\vec{Z}_i; \vec{r}_i^\alpha\}) \rangle}{\langle \Phi(\{\vec{Z}_i; \vec{r}_i^\alpha\}) | \Phi(\{\vec{Z}_i; \vec{r}_i^\alpha\}) \rangle}.$$

In the case of a two-body force, the Hamiltonian operator is given by the following form;

$$\hat{H} = \sum_{k=1}^{4N} \hat{t}_k - T_{c.m.} + \sum_{k>l}^{4N} \hat{v}_{kl} + \sum_{k>l}^{4N} \frac{(1 + \tau_z(k))(1 + \tau_z(l)) e^2}{4r}, \quad (5)$$

where the first and the second terms present the kinetic energy dropping out the center of mass motion energy. The third and fourth terms are nuclear and Coulomb two-body interactions, respectively. Solving Eq.(4) is just a variational technique to search for a set of  $\{\vec{Z}_i\}$  which give a lower energy state as  $\beta$  increases, and this process can be physically interpreted as a dynamical friction cooling process.<sup>17, 18)</sup> It is easy to show that  $\beta$  derivative of  $\mathcal{H}$  becomes negative:

$$\begin{aligned} \frac{d\mathcal{H}}{d\beta} &= \sum_{i=1} \frac{\partial \mathcal{H}}{\partial \vec{Z}_i} \cdot \frac{d\vec{Z}_i}{d\beta} + \sum_{i=1} \frac{\partial \mathcal{H}}{\partial \vec{Z}_i^*} \cdot \frac{d\vec{Z}_i^*}{d\beta} \\ &= -2 \sum_{i=1} \frac{d\vec{Z}_i^*}{d\beta} \cdot \frac{d\vec{Z}_i}{d\beta} \leq 0. \end{aligned} \quad (6)$$

The expectation value of the Hamiltonian decreases and the nucleus is cooled as  $\beta$  increases. In general, since the resultant cooled state  $\Phi(\{\vec{Z}_i; \vec{r}_i^\alpha\})$  is not the eigenstate of an angular momentum, we have to project it to  $\Phi^{lm}(\{\vec{Z}_i; \vec{r}_i^\alpha\})$ ;

$$\Phi^{lm}(\{\vec{Z}_i; \vec{r}_i^\alpha\}) = \frac{2l+1}{8\pi^2} \int d\Omega D_{mK}^{l*}(\Omega) \hat{R}(\Omega) \Phi(\{\vec{Z}_i; \vec{r}_i^\alpha\}), \quad (7)$$

where  $\Omega$  is the Euler angle of  $\{\vec{r}_i^\alpha\}$ . In the numerical integration over the Euler angle  $\Omega(\alpha, \beta, \gamma)$ , we have adopted (25)<sup>3</sup> mesh points and the integration is carried out with the Gauss-Legendre integral technique. The intrinsic angular momentum component  $K$  is chosen to be zero for simplicity.

The state obtained by the angular momentum projection from the energy minimum configuration gives merely an approximate ground state in the sense of the projection after variation (PAV). Our model function is cooled before the angular momentum projection. However, we will construct the wave function by superposing many different intrinsic states (GCM). We provide GCM basis wave functions with many single-Slater determinants obtained by the cooling method. Then we expect that the PAV approximation does not give rise to a serious problem for the final wave function. This problem of PAV approximation and the effect of superposing many states will be discussed quantitatively later in detail.

### 2.3 Superposition of different intrinsic states

The more reliable wave function  $\Psi^{lm}(\{\vec{r}_i^\alpha\})$  should be expressed by a linear combination of many different intrinsic states  $\Phi_i^{lm}(\{\vec{Z}_i; \vec{r}_i^\alpha\})$ ;

$$\Psi^{lm} = \sum_j c_j \Phi_j^{lm}. \quad (8)$$

The GCM basis wave functions  $\{\Phi_j^{lm}\}$  are not necessary to be orthogonal with each other. The energy spectra are calculated by diagonalizing the Hamiltonian and overlap matrices, namely by solving the Hill-Wheeler equation;

$$\sum_k (\langle \Phi_j^{lm} | H | \Phi_k^{lm} \rangle - E \langle \Phi_j^{lm} | \Phi_k^{lm} \rangle) c_k = 0. \quad (9)$$

We prepare many different intrinsic states  $\Phi^{lm}(\{\vec{Z}_i; \vec{r}_i^{\alpha}\})$  by using the constraint cooling method,<sup>18)~21)</sup> by which we can search for a set of suitable complex parameters  $\{\vec{Z}_i\}$  to minimize the expectation value of the energy under some constraints. In our framework, we constrain the expectation value of the principal quantum numbers  $n_x$ ,  $n_y$  and  $n_z$  of the harmonic oscillator. Of course in this framework we can also constrain other physical values, for example an angular momentum. However, cooling with an angular momentum constraint essentially results in giving the rotating nucleus with a similar intrinsic state when the angular momentum is not so high. Then these states are not very effective as GCM basis states.

The constraint cooling is carried out as follows: First we prepare an initial state of the cooling satisfying the given constraint condition. As an example, when the given constraint is  $(n_x, n_y, n_z) = (a, b, c)$ , we consider the following function  $f$  which expresses a gap between expectation value and desirable constraint values;

$$f = (n_x - a)^2 + (n_y - b)^2 + (n_z - c)^2 . \quad (10)$$

For this  $f$ , we solve the following cooling-like equation;

$$\frac{d\vec{Z}_i}{d\beta} = -\frac{\partial f}{\partial \vec{Z}_i^*}, \text{ and c.c. .} \quad (11)$$

These equations also satisfy the condition  $df/d\beta \leq 0$ , and therefore  $f$  decreases as  $\beta$  evolves. When the value of  $f$  becomes nearly equal to zero and the wave function satisfies the desirable constraint condition, we go to the second step.

Following Ref. <sup>19)</sup>, we next cool the nucleus keeping the constraint condition by solving the constraint cooling equation given by

$$\frac{d\vec{Z}_i}{d\beta} = -\frac{\partial \mathcal{H}}{\partial \vec{Z}_i^*} - \sum_{l=1} \eta_l \frac{\partial \langle W_l \rangle}{\partial \vec{Z}_i^*}, \text{ and c.c. ,} \quad (12)$$

where,  $\eta_l$  is the Lagrange multiplier and  $W_l$  is an expectation value of the constrained observable, here  $W_l = \hat{n}_x, \hat{n}_y$  and  $\hat{n}_z$ . If the constraint condition  $d \langle W_l \rangle / d\beta = 0$  is satisfied, these equations provide the condition  $d\mathcal{H}/d\beta \leq 0$ , and we can cool the nucleus. Here we define  $\eta_l$  so as to satisfy the condition  $d \langle W_l \rangle / d\beta = 0$ , which is rewritten as

$$\begin{aligned} & \frac{d \langle W_l \rangle}{d\beta} \\ &= \sum_{i=1} \left\{ \frac{\partial \langle W_l \rangle}{\partial \vec{Z}_i} \cdot \frac{d\vec{Z}_i}{d\beta} + \frac{\partial \langle W_l \rangle}{\partial \vec{Z}_i^*} \cdot \frac{d\vec{Z}_i^*}{d\beta} \right\} \\ &= -2\Re \sum_{i=1} \left\{ \frac{\partial \langle W_l \rangle}{\partial \vec{Z}_i} \cdot \left( \frac{\partial \mathcal{H}}{\partial \vec{Z}_i^*} + \sum_{m=1} \eta_m \frac{\partial \langle W_m \rangle}{\partial \vec{Z}_i^*} \right) \right\} \\ &= 0 . \end{aligned} \quad (13)$$

Defining the following vector and matrix;

$$G_l = \Re \sum_{i=1} \frac{\partial \langle W_l \rangle}{\partial \vec{Z}_i} \cdot \frac{\partial \mathcal{H}}{\partial \vec{Z}_i^*} , \quad (14)$$

$$F_{lm} = \Re \sum_{i=1} \frac{\partial \langle W_l \rangle}{\partial \vec{Z}_i} \cdot \frac{\partial \langle W_m \rangle}{\partial \vec{Z}_i^*} , \quad (15)$$

we express the last equality of Eq.(13) as

$$G_l + \sum_m \eta_m F_{lm} = 0 . \quad (16)$$

Therefore, the Lagrange multiplier  $\eta_l$  is expressed by

$$\eta_l = - \sum_k G_k F_{lk}^{-1} . \quad (17)$$

## 3 Results of $^{12}\text{C}$ and $^{16}\text{O}$

### 3.1 Approximation of projection after variation

To see a reliability of our model and also the approximation which comes from PAV, we compare the ground state energy of our model for  $^{12}\text{C}$  with the  $3\alpha$  RGM calculation by Fukushima and Kamimura.<sup>2)</sup> For this purpose, we employ the same parameters for the  $NN$  interaction, that is the Volkov interaction<sup>22)</sup> (Table I) with the Majorana exchange parameter  $M = 0.59$  and the size parameter  $\nu=0.275 \text{ fm}^{-2}$  of the wave function. The Coulomb interaction is also included.

Table I

The ground state energy obtained by the  $3\alpha$  RGM is -89.4 MeV, which corresponds to the binding energy of 7.3 MeV from the  $3\alpha$  threshold. These results are in good agreement with the experimental data. As a result of cooling, we obtain the  $^{12}\text{C}$  energies of -74.5 MeV and -86.2 MeV for the intrinsic state and  $0^+$  projected state, respectively. The large difference between results of the cooling and of the RGM implies that the cooled state contains components of many different angular momenta. This can be understood from the fact that the angular momentum projection effect is very large. The 3.2 MeV difference between PAV and RGM suggests that the PAV gives a rather good approximation but not necessarily brings an exact ground state within the  $\alpha$ -cluster model.

We show, in Fig.1, the  $3\alpha$  energy surface obtained by cooling with the constrained principal quantum number. The intrinsic  $3\alpha$ -cluster wave functions are characterized by two dimensional principal quantum numbers  $(n_y, n_z)$  by fixing  $n_x = 0$ . The wave functions specified by  $(n_y, n_z)$  might have correspondence to some basic shell model configurations; the  $SU_3$   $(\lambda, \mu)=(0, 4)$  state is expressed with the principal quantum number  $n=8$  which corresponds to the minimum value because of the antisymmetrized wave function. The wave function with  $n_x=0$  and  $n_y=0$  represents a linear chain configuration whose minimum oscillator quantum number is 12 corresponding to the  $(0s)^4(z)^4(z^2)^4$  shell model state.

Fig.1

Fig.2

From Fig.1 of the energy surface, we can see which configuration gives a more stable structure. We find the lowest energy point at the total principal quantum number  $n (=n_y+n_z)=9.6$  which deviates a little from the lowest shell model configuration. The lowest energy point also lies at  $n_y = n_z$  of the diagonal line which expresses a equilateral triangle configuration. The valley of the energy surface extends to the direction of  $n_z > n_y$  or  $n_y > n_z$ . This property of the energy surface implies that the equilateral triangle configuration at the lowest point changes to a non-equilateral triangle one in higher energies.

In Fig.2, we display the energy surface projected to the angular momentum  $0^+$  from each state in Fig.1. The energy minimum point seen at  $n = 10.5$  moves from that in Fig.1. This result indicates that the angular momentum projection after the constraint cooling procedure provides a lower energy which is about 1 MeV deeper than that of PAV, and an enhancement of clustering. However, the lowest energy -87.2 MeV in Fig.2 is still higher than the results of the RGM. This under-binding by about 2 MeV from the RGM result would be due to the angular momentum projection from a single intrinsic configuration.

In order to improve the energy of the  $3\alpha$  system, we take superposition of many intrinsic states. The more realistic ground state might be expressed by superposition of wave functions

around the energy minimum of the energy surface. We solve the energy and the amplitudes of a linear combination of the  $0^+$  wave function projected from every cooled intrinsic state by using a framework of GCM. In this framework, we can solve not only the ground state but also excited states simultaneously. To obtain excited states corresponding to the observed  $0_2^+$  state at 7.65 MeV in  $^{12}\text{C}$ , we have to choose GCM basis states appropriately.

### 3.2 GCM and convergence of the ground state energy

We employ 30 GCM basis states obtained by the constraint cooling method, where the intrinsic configurations are specified by the quantum number  $(n_y, n_z)$ . Here we should notice that the values of  $n_y$  and  $n_z$  are not eigenvalues but expectation values. Therefore, they are taken to be not necessarily integers, especially for  $(n_y, n_z)$  near the forbidden region. In this process, we also introduced a constraint

$$\langle \sum_i a_y^\dagger(i) a_z(i) \sum_j a_z^\dagger(j) a_y(j) \rangle / n \leq 1 \quad (18)$$

to obtain intrinsic states with the maximum weight of  $SU_3$ , where  $\bar{a}^+(i)$  ( $\bar{a}(i)$ ) is an creation (annihilation) of the  $i$ -th particle harmonic oscillator and  $n$  is the expectation value of the total oscillator quanta. To see the ground state energy convergence, we prepare two kinds of GCM basis sets. As set I, we choose an appropriate selection of  $(n_y, n_z)$  configurations around the energy minimum region. Set II is given by  $(n_y, n_z)$  configurations corresponding to the  $SU_3$  Pauli-allowed states of the  $3\alpha$  system with  $n \leq 15$ . In Table II, we present the employed  $(n_y, n_z)$  configurations of sets I and II.

Table II

The ground  $0^+$  state energy convergence are displayed in Fig.3 and Fig.4. The energies calculated with both basis sets converge to -89.4 MeV which is the same value as the  $3\alpha$  RGM. This result indicates that the present AMD+GCM framework works very successfully. In set I, we took several  $(n_y, n_z)$  configurations with larger values of  $n$  as GCM basis states. These basis states give little contribution to the ground  $0^+$  state but rather large effects on the excited solution such as the second  $0^+$  state.

Fig.3

Fig.4

In the previous subsection, we found that the PAV calculation to get the good parity and angular momentum state gave a little small binding energy of the  $3\alpha$  ground state in comparison with the RGM result. However, from the present result, we can consider that such a defect of PAV is well recovered by the GCM calculation. We further apply this method to the  $4\alpha$  system.

### 3.3 Results of the $4\alpha$ model for $^{16}\text{O}$

We have shown that when we use the Majorana exchange parameter  $M = 0.59$ , the binding energy of  $^{12}\text{C}$  is reasonably reproduced. However, if we use this parameter, we obtain a too large binding energy of  $^{16}\text{O}$ , which is more than 152 MeV and corresponds to an over-binding more than 25 MeV. In addition, the  $0_2^+$  state of the  $4\alpha$  system is not reproduced at the  $^{12}\text{C}+\alpha$  threshold. These results suggest that we must change the Majorana exchange parameter in a calculation of  $^{16}\text{O}$ .

When the effective  $NN$  interaction used is the Volkov No.2 with the Majorana exchange parameter  $M = 0.63$  and the size parameter  $\nu=0.23 \text{ fm}^{-2}$ , we obtain a reasonable binding energy of  $^{16}\text{O}$ . However, we have to take a superposition of some  $4\alpha$  configuration as the GCM basis states in order to get the well converged solutions. The  $^{16}\text{O}$  ground state is expected to have a doubly closed-shell configuration which is expressed by the  $SU_3 (\lambda, \mu)=(0,0)$  state. On the other hand, the excited  $0^+$  states might have the  $^{12}\text{C}+\alpha$  clusterized configuration. Therefore, we choose the GCM basis states which is close to the  $(\lambda, \mu) = (0, 0)$  configuration for lower  $n = (n_x + n_y + n_z)$  values and many states including the  $^{12}\text{C}+\alpha$  configurations with higher  $n$  values. In Table III, we show the employed  $(n_x, n_y, n_z)$  configurations.

Table III

By using 30 GCM basis states, we calculate the energy convergence of the  $0^+$  states. The results are presented in Fig.6. It is shown that the ground  $0^+$  state energy well converges within a small number of basis states but the convergence of the second  $0^+$  state energy is very gentle. To obtain a well-converged result of the second  $0^+$  state, we have to employ a rather large number of GCM basis states including higher values of  $n$ . These results support our consideration of the  $^{16}\text{O}$  ground state and excited state structure mentioned above.

Fig.5

The calculated ground state energy is  $-127.6 \text{ MeV}$  and almost the same as the experiment. However the second  $0^+$  state is obtained at  $-109.2 \text{ MeV}$ . The excitation energy of the  $0_2^+$  state is  $18 \text{ MeV}$  which is very different from the observed  $6.05 \text{ MeV}$ . This discrepancy comes from the fact that the binding energy of  $^{12}\text{C}$  is never reproduced with the present exchange parameter  $M = 0.63$  of the Volkov No.2 force. This case gives only  $-82.0 \text{ MeV}$  for  $^{12}\text{C}$ . The energy of the  $0_2^+$  state is obtained just around the  $^{12}\text{C}+\alpha$  threshold energy  $-109.4 \text{ MeV}$  (B.E. $(^{12}\text{C}) = 82.0 \text{ MeV}$  and B.E. $(\alpha) = 27.4 \text{ MeV}$ ).

This result is very interesting, because the similar situation has been reported in the  $^{12}\text{C}+\alpha$  RGM study by Horiuchi.<sup>8)</sup> His calculation where the  $^{12}\text{C}(0,4)+\alpha$  model space is assumed has been done with  $M = 0.67$  of the Volkov No.2 force. This exchange parameter has been chosen so as to reproduce the  $0_2^+$  state around the  $^{12}\text{C}+\alpha$  threshold, but it gives much smaller binding energies by about  $20 \text{ MeV}$  for both  $^{12}\text{C}$  and  $^{16}\text{O}$ . The present calculation of the  $4\alpha$  model, which has no assumption of the  $^{12}\text{C}+\alpha$  configuration, well reproduces the binding energy of the  $^{16}\text{O}$  ground state and reasonably the  $0_2^+$  state around the  $^{12}\text{C}+\alpha$  threshold energy.

### 3.4 Density dependent forces and other force

In the previous section, we have found that the binding energies of both  $^{12}\text{C}$  and  $^{16}\text{O}$  nuclei are not consistently reproduced simultaneously within the two-body effective interaction Volkov No.2. This defect may partially come from the nature of the interaction used, which does not satisfy the saturation property of nuclear matter. Thus, we use effective interactions satisfying the saturation property. Here, we have used the Skyrme II force,<sup>26)</sup> the Tohsaki No.1 force,<sup>24)</sup> and Brink-Boeker No.1 force.<sup>27, 28)</sup> The first two interactions have repulsive three-body terms which cause the density dependence of the effective interaction. The last one has only two-body terms with large exchange mixture.

For these interactions, we have adopted the parameters as shown in Table IV. Note that the size parameter  $\nu$  for the Skyrme II force is chosen to be smaller than those used for other

interactions. The dependence on  $\nu$  is very large in the case of the Skyrme interaction, then we have selected around the value giving the almost maximum binding energy of  $\alpha$  and  $^{12}\text{C}$ .

Table IV

The results calculated with these three interactions are summarized in Table V. We show the ground state energies of  $\alpha$ ,  $^{12}\text{C}$  and  $^{16}\text{O}$  and the second  $0^+$  state of  $^{16}\text{O}$ . The previous results with the Volkov No.2 force is also shown in the table. From these results, we find that, except for the B-B No.1 force, the binding energies of  $^{16}\text{O}$  is reasonably reproduced within about 3 MeV, and the excited second  $0^+$  state appears around the  $^{12}\text{C}+\alpha$  threshold. This fact suggests that the physical picture for the  $0_2^+$  state of  $^{16}\text{O}$  — a  $^{12}\text{C}+\alpha$  cluster state — is well justified when a large functional space is adopted and a reasonable binding energy of  $^{16}\text{O}$  is given. However, the binding energy of  $^{12}\text{C}$  is calculated to be too small with all the interaction used compared with the experimental data. Therefore the binding energy difference between  $^{12}\text{C}$  and  $^{16}\text{O}$  is still larger, although the Tohsaki No.1 force gives a little less difference. Thus we have to say that the binding energy problem is still unsolved. We will discuss this problem in the next section.

Table V

The energy levels calculated with the Volkov No.2 force and the Tohsaki No.1 force are shown in Figs.6 and 7 for  $^{16}\text{O}$  and  $^{12}\text{C}$ , respectively. The present GCM results are similar to those of previous works<sup>2, 8, 29)</sup>, and coincides with the experimental energy levels qualitatively, except the ground state of  $^{16}\text{O}$ . Namely, all the observed low-excited levels appear in that energy region within about 3 MeV (except an unnatural parity states such as a  $2^-$  states in  $^{16}\text{O}$ ), and the order of the lower levels is reproduced when the states of each parity are separately considered.

Fig.6

Fig.7

## 4 Discussion

In this section, first we would like to discuss the reliability of our model by comparing it with those used in other works. Next, we would like to discuss what is expected to be important to solve the binding energy problem of  $^{12}\text{C}$  and  $^{16}\text{O}$ .

### 4.1 Comparison with Other Works

Recently, Kanada-En'yo, Horiuchi and Ono have applied the cooling method to the AMD wave functions of  $^{20}\text{Ne}$  <sup>19)</sup> and neutron-rich nuclei.<sup>20, 21)</sup> For example, they have discussed the  $^{20}\text{Ne}$  structure change along the yrast line states qualitatively, by carrying out cooling with a constraint of an angular momentum and projecting afterwards from this single Slater-determinant into the  $J^\pi$  state (PAV). In their work, where any cluster configuration is not assumed apriorily, they can study appearance of an  $^{16}\text{O}+\alpha$  cluster configuration in the ground rotational band, the dissolution of  $\alpha$ -cluster at  $8^+$ , and appearance of a  $^{12}\text{C}+\alpha+\alpha$  configuration at  $10^+$  and  $12^+$ . It is very interesting and challenging to investigate nuclear structure over wide mass number range by using such a wave function which consists of many degrees of freedom, and the AMD wave functions are expected to be qualitatively reliable. In fact, we have already shown that the cooled and  $J^\pi$ -projected (PAV) wave function gives less ground state binding energies by only about 2 and 1 MeV for  $^{12}\text{C}$  and  $^{16}\text{O}$ , respectively. This energy difference is not very serious for the systematic study over wide mass number region. However, we have to point out that the superposition effects of various intrinsic states in GCM is essential for the understanding of higher nodal states such as the second  $0^+$  states, in which  $3\alpha$  ( $^{12}\text{C}$ ) and  $^{12}\text{C}+\alpha$  ( $^{16}\text{O}$ ) configurations appear. On the other hand, it is very time-consuming and not very effective to carry out GCM calculation for the study of these states with the full AMD wave functions, in which all the nucleonic degrees of freedom are accounted for. This is the main reason why we have assumed the  $\alpha$ -cluster wave function, instead of using the full AMD wave function.

Recently, Descouvemont has investigated  $^{16}\text{O}$  structure with a microscopic  $4\alpha$  model.<sup>29)</sup> In his work,  $^{12}\text{C}(0^+, 2^+)+\alpha$  configuration is adopted and it is assumed that this  $^{12}\text{C}$  nucleus have equilateral triangle  $3\alpha$  configurations. As for the effective interaction, the Volkov No.2 interaction with Majorana exchange parameter  $M = 0.6305$  is used. This parameter is fitted to reproduce the energy of the first  $2^+$  state from  $^{12}\text{C}+\alpha$  threshold. While we have fixed the value of  $M = 0.63$  to reproduce the ground state binding energy of  $^{16}\text{O}$ , it coincides fairly well with each other. Thus, our results with the Volkov No.2 interaction are very similar to those in Ref. <sup>29)</sup>. For example, the binding energy of  $^{16}\text{O}$  from the  $^{12}\text{C}+\alpha$  threshold is calculated to be about 18 MeV, and the second  $0^+$  state appears around the threshold. The main difference between his work and ours lies in the assumed configuration space. We would like to emphasize that the second  $0^+$  state appears around the  $^{12}\text{C}+\alpha$  threshold in our  $4\alpha$  model without assuming the configuration of  $^{12}\text{C}+\alpha$ . We consider that this coincidence strongly supports the picture of the  $^{12}\text{C}+\alpha$  model especially for the excited states of  $^{16}\text{O}$ . The second difference is in the way of  $J^\pi$  projection. Our model is based on the strong coupling picture and  $J^\pi$  projection is carried out only once. On the other hand, in his calculation, the  $J^\pi$  projection is performed through two steps: First, the  $^{12}\text{C}$  wave function in  $^{16}\text{O}$  is projected to  $0^+$  and  $2^+$  states, and later the total wave function of  $^{12}\text{C}+\alpha$  is projected to given total  $J^\pi$  states. This difference can affect the level structure, especially for those states in which the distance between  $^{12}\text{C}$  and  $\alpha$  becomes large and the weak coupling picture is

valid. Our results support his calculation and suggest that this effect can also be taken into account by employing many different states as the GCM basis states in our framework.

## 4.2 Effects of Clustering and GCM

In this work, we have incorporated the effects of the clustering (constraint cooling),  $J^\pi$  projection, and the configuration mixing (GCM). In order to see the combined effects of clustering and GCM, we show in Table VI the comparison of the GCM results with the  $SU_3$  limit calculation<sup>24)</sup> as an example. In Ref.<sup>24)</sup>, Tohsaki calculated the binding energy of  $^{12}\text{C}$  and  $^{16}\text{O}$  within the shell-model  $SU_3$  limit;  $(\lambda, \mu)=(0, 4)$  for  $^{12}\text{C}$  and  $(\lambda, \mu)=(0, 0)$  for  $^{16}\text{O}$ . Then the  $^{12}\text{C}$  ground state energy is calculated to be -75.2 MeV which is shorter by about 17 MeV than the experiment. From this large under-binding, he has suggested that the  $\alpha$ -cluster model may be invalid for  $^{12}\text{C}$ , however, we have shown that the ground state energy of  $^{12}\text{C}$  is largely improved after taking the clustering effects into account.

Table VI
----------

While it is already pointed out in many previous studies that the clustering and the GCM effects are very large in  $^{12}\text{C}$  within two-body interactions, we show in this paper that this point is valid also with three-body interactions. Although these effects contribute smaller for the ground state of  $^{16}\text{O}$  which has been believed to have mainly the doubly closed-shell configuration ( the  $SU_3(\lambda, \mu)=(0, 0)$  configuration), the clustering and the GCM effect is about 8 MeV and can be hardly neglected.

Between these two effects of clustering and GCM, the former is shown to be larger within the present GCM, at least when only the ground state energy is addressed. For example for  $^{16}\text{O}$ , the difference between the shell model limit configuration and the energy minimum state on the  $J^\pi$ -projected surface (  $(n_x, n_y, n_z) \simeq (5, 5, 5)$  ) is around 6 MeV for  $^{16}\text{O}$  in our calculation (Volkov No.2 with  $M = 0.63$ ), while the difference is about 10 MeV for  $^{12}\text{C}$ . Once a energy minimum state on the  $J^\pi$ -projected surface is selected, the GCM effects on the ground state binding energy is about 2 MeV and 1 MeV for  $^{12}\text{C}$  and  $^{16}\text{O}$ , respectively. Needless to say, the main effects of GCM appear in the excited states; we need more than 15 GCM basis states to describe  $0_2^+$  states of  $^{12}\text{C}$  and  $^{16}\text{O}$  (see Figs. 3, 4 and 5). Even for the yrast line states, the energy gets lower by about 2 MeV in the case of the  $2^+$  state of  $^{12}\text{C}$  compared with PAV results.

Finally, we have to mention about the importance of the  $J^\pi$  projection. Without  $J^\pi$  projection, we cannot discuss the absolute energy and the stable configurations in the excited states. Fig.1 and Fig.2 show that, in addition to the large energy gain by the  $J^\pi$  projection procedure more than 10 MeV, the shape of the energy surface is largely modified. Thus, especially in the excited state, it is almost impossible to distinguish which configuration has low energy from the before-projected energy surface.

## 4.3 Tohsaki Force in an $\alpha$ -Cluster Model

The resultant energy levels obtained by using the Volkov No.2 force with the Majorana exchange parameter  $M = 0.63$  and the Tohsaki force are very similar. However, we have found that there are some evidences that the Tohsaki force gives more reasonable result than those of the Volkov No.2 force. First of all, the energy difference between  $^{12}\text{C}$  and  $^{16}\text{O}$  is smaller by about 2 MeV in the case of the Tohsaki force than the Volkov No.2 force. At the

same time, the Tohsaki force gives the  $^{12}\text{C}$  binding energy 5 MeV from the  $3\alpha$  threshold, which corresponds to be about 2 MeV underbound but much reasonable than the result of using the Volkov No.2 force.

Then, this density dependent interaction (the Tohsaki force) contribute to the quantitative reliability of describing these nuclei by our model. However, one of the defects is an over-binding of  $^{16}\text{O}$ . The resultant ground state energy is lower by about 3 MeV than the experimental data. Although this force has no free parameter, it seems to be necessary to modify some parameters of this force to reproduce the energy levels of  $^{16}\text{O}$  *after GCM*. In our preliminary results, we have found that the binding energy difference between  $^{12}\text{C}$  and  $^{16}\text{O}$  can be reduced by a few MeV after modifying the strength of the middle range two- and three-body terms in the Tohsaki No.1 force.

Although it has been expected that the binding energy problem can be solved with density dependent forces, we have shown that the problem still remains unsolved even if we use effective interactions with density dependence. Therefore in order to solve this binding energy problem, we have to incorporate some other mechanisms which contribute larger to the binding energy of  $^{12}\text{C}$  than that of  $^{16}\text{O}$ . A hint of solving this problem can be seen in the energy levels of  $^{12}\text{C}$ . With both of the Volkov No.2 and the Tohsaki No.1 force, the energies of  $2^+$  and  $4^+$  states are calculated to be lower than the experimental data. In the harmonic oscillator shell model for  $^{12}\text{C}$ , the kinetic energies of the ground state and these  $2^+$  and  $4^+$  states are the same, then the excited energies must come from the interaction. Since the central forces are not enough to explain this energy difference between calculations and experiments, it might come from spin dependent interactions such as the  $ls$  force. This speculation is also supported from the shell model picture, since the  $p_{3/2}$  single particle states are filled in  $^{12}\text{C}$  and these states get more binding from the  $ls$  interaction. However, as we already mentioned, the cluster model description is better for  $^{12}\text{C}$  than a shell model description, and the above expectation is not trivial. In order to clarify this point, we have to take the  $ls$  force effects into account within the cluster model, in which the break-up of  $\alpha$ -cluster is incorporated, since the matrix elements of the  $ls$  force vanish in  $\alpha$ -cluster wave functions.

## 5 Summary and Conclusion

We have studied the structure of  $^{12}\text{C}$  and  $^{16}\text{O}$  by using the constraint cooling method and GCM with various two- and three-body interactions. One of the goals of this study is to solve the well-known binding energy problem of these nuclei.

It has been a long-standing problem that the binding energies of both of  $^{12}\text{C}$  and  $^{16}\text{O}$  nuclei cannot be reproduced simultaneously by using the same effective interaction within fully microscopic models; *i.e.* the binding energy difference between  $^{12}\text{C}$  and  $^{16}\text{O}$  is calculated to be much larger than the experimental data. There have been a lot of discussions on the origin of this binding energy problem. One of the difficulties to solve this problem comes from the necessity of a large functional space; even if we limit the wave function space to that of the  $\alpha$ -cluster model, we have to solve three- and four-body problem. Thus, in many of previous works, while the  $^{12}\text{C}$  nucleus is treated in the  $3\alpha$ -cluster model space, only the two-body configuration of  $^{12}\text{C}+\alpha$  is assumed for the  $^{16}\text{O}$  nucleus<sup>8, 9, 10</sup>). Therefore, the excitation or the dissolution of  $^{12}\text{C}$  in  $^{16}\text{O}$ , which is expected to make the binding energy difference smaller, has been hardly discussed within fully microscopic models. Another probable origin is the effects which comes from the density dependent interaction. Since  $^{16}\text{O}$  is believed to be well expressed by the doubly closed-shell configuration, the density in  $^{16}\text{O}$  is considered to be higher than that in  $^{12}\text{C}$ . Thus the binding energy difference may become smaller if we have included the effects of density dependent interactions. Until now, however, it has been difficult to treat density dependent interactions in a larger functional space than a single Slater determinant.

In order to solve or clarify the origin of this problem, we have introduced a new method based on the constraint cooling method and Generator Coordinate Method (GCM) within the  $N\alpha$ -cluster model space. This method is regarded as a combined framework of projection after variation (PAV) and variation after projection (VAP). In the first step, we prepare the GCM basis states by applying the constraint cooling method, which has been developed in Antisymmetrized Molecular Dynamics (AMD)<sup>17</sup>), and project the wave function to a  $J^\pi$  eigenstate. This process corresponds to PAV since the variation is calculated in an intrinsic configuration. The obtained intrinsic states are expected to contribute to the low-lying states including the ground state, since we can generate various intrinsic states with constraints which have low expectation values of the Hamiltonian. In the second step, the GCM diagonalization is performed within the  $J^\pi$ -projected model space (VAP); *i.e.*, the contribution from different intrinsic configurations to each excited state is taken into account by the variation in the  $J^\pi$  eigenstates. By these double variation procedures, we expect that this model gives more reliable wave functions of many levels. In addition, this model has another merit that we can easily use a density dependent force expressed by a three-body interaction. Since the GCM basis states used here are the Slater determinants consisting of Gaussian wave packets, the matrix elements between the intrinsic states are given by analytic expressions. Thus, as for the numerical integrations, only we need is those over the Euler angle to get the matrix elements between  $J^\pi$ -projected basis states.

First, we have studied the energy spectra of the  $3\alpha$  system for which many reliable model calculations exist in order to check the reliability of this model. The interaction used here is the Volkov force with the Majorana exchange parameter  $M = 0.59$ . As the constraint parameters which are regarded as the generator coordinates of the model, we have chosen principal quantum numbers for each direction. From the energy surface of  $n_z$  and  $n_y$ , we have found that the results of PAV (cooling and projection) and partial VAP (selecting the

energy minimum state on the  $0^+$ -projected plane) show about 3 MeV and 2 MeV under-binding for the ground state compared with the results by Fukushima and Kamimura<sup>2)</sup>, respectively. After GCM, the calculated binding energy and excited energy spectra within this model are quantitatively consistent with those of Refs.<sup>2)~4)</sup>. These results show that the effects of GCM is fairly large for the quantitative description of the energy spectra since the binding energy of  $^{12}\text{C}$  from the  $3\alpha$  threshold is only 7.3 MeV. We have also found that the ground state binding energy convergence is very rapid; it converges with about 10 basis states within 300 keV, and this feature does not strongly depend on how to choose the GCM basis states (the constraints in the cooling process), if the total principal quantum number is chosen in the range around from 8 to 13.

Next we have investigated the  $4\alpha$  system, and discussed the origin of the binding energy problem. Now the first problem here is which interaction should be used for the consistent understanding of  $^{12}\text{C}$  and  $^{16}\text{O}$ . If we use the effective interaction with the same parameter as that in the previous  $3\alpha$  case ( $M = 0.59$ ), the calculated results show a too large binding energy for the ground state and undesirable level structure of  $^{16}\text{O}$ . Since we are trying to understand the binding energy problem including their absolute binding energies by extending the model space, the over-binding cannot be remedied without changing the interaction. *i.e.* we must avoid  $^{16}\text{O}$  from being overbound. In the previous work by Horiuchi,<sup>8)</sup> the Volkov No. 2 force with  $M = 0.67$  is adopted to reproduce the second  $0^+$  state of  $^{16}\text{O}$  near the  $^{12}\text{C}+\alpha$  threshold within the  $^{12}\text{C}+\alpha$  RGM. However, since our model space is much larger than that in the above RGM, using  $M = 0.67$  no more reproduces the  $0_2^+$  state around the threshold in our model. Furthermore, the absolute binding energies of both nuclei are calculated to be too small with this interaction. Therefore, we have decided to use the Volkov No.2 force with the common Majorana exchange parameter  $M = 0.63$  in both  $^{12}\text{C}$  and  $^{16}\text{O}$ , which gives a reasonable absolute binding energy for  $^{16}\text{O}$  (127.6 MeV). With this interaction, the second  $0^+$  state of  $^{16}\text{O}$  is calculated to be around  $^{12}\text{C}+\alpha$  threshold, which agrees with the  $^{12}\text{C}+\alpha$  picture for this level. However, the energy difference between the first and the second  $0^+$  states is much larger than the experiment by about 12 MeV which comes from the underestimate of the binding energy of  $^{12}\text{C}$  (82.0 MeV).

The above results suggest that if the binding energy of  $^{12}\text{C}$  is reasonably reproduced and a large model space as in this work is adopted, we can consistently understand the energy spectra both of  $^{12}\text{C}$  and  $^{16}\text{O}$ . Then, it is necessary to take into account another mechanism for reasonable description such as the density dependence of the effective interaction. The density dependent interactions are expected to behave more repulsively for  $^{16}\text{O}$  than for  $^{12}\text{C}$ , and to decrease the binding energy difference. Thus, we have applied our model to the  $3\alpha$  and  $4\alpha$  problem using density dependent interactions; the zero-range Skyrme interaction and the recently-proposed Tohsaki force with finite range three-body terms. Applying these interactions shows very similar results as those with the Volkov No.2 interaction ( $M = 0.63$ ). Namely, the absolute binding energy of  $^{16}\text{O}$  is well reproduced but  $^{12}\text{C}$  becomes underbound. Furthermore, the second  $0^+$  state of  $^{16}\text{O}$  appears around the  $^{12}\text{C}+\alpha$  threshold. The binding energy difference between  $^{12}\text{C}$  and  $^{16}\text{O}$  becomes a little smaller compared with that of the Volkov No. 2 force, however, the binding energy problem is not fully solved yet.

In summary, we have investigated the energy spectra both of  $^{12}\text{C}$  and  $^{16}\text{O}$  within the  $\alpha$ -cluster model. First we have applied our model to  $^{12}\text{C}$  and shown that this model gives the same binding energy as the RGM calculation by Fukushima and Kamimura<sup>2)</sup>. Next, we have also applied it to the  $4\alpha$  system. In our model, the second  $0^+$  state of  $^{16}\text{O}$  has been reproduced around the  $^{12}\text{C}+\alpha$  threshold, when the absolute binding energy of  $^{16}\text{O}$  is well

reproduced, and this feature is common to various effective interactions. It is very significant that the resultant excited energy levels agree with the physical picture suggested by the Ikeda diagram. From the results of the calculations by these many kinds of interactions, however, the binding energy problem remains unsolved, although we have used a very large functional space and various effective two- and three-body interactions. Therefore we conclude that the binding energy problem between  $^{12}\text{C}$  and  $^{16}\text{O}$  can not be solved only with the density dependent interactions. In order to solve this binding energy problem, we have to incorporate some other mechanism which does not contribute to the binding energy of  $^{16}\text{O}$  but contributes to  $^{12}\text{C}$ . One of the probable way is to take into account the contribution of the  $ls$  force whose effects vanish in  $\alpha$ -cluster model wave functions. For this purpose, we have to extend our model space to include configurations such as  $2\alpha + 3N + N$  for  $^{12}\text{C}$ . Such  $(3N + N)$  configurations are known to contribute to high excited states of  $^8\text{Be}^{30)}$  or  $^9_{\Lambda}\text{Be}^{31)}$ . We expect that these effects of [4]-symmetry breaking on the ground state of  $^{12}\text{C}$  is much larger than that on  $^{16}\text{O}$ , since the  $ls$  splitting makes the  $p_{3/2}$  single particle energy lower.

The authors greatly thank to Professor S.Okabe and Professor K.Ikeda for useful discussions, and also to Mr. Y.Nara who has been supporting our study very much especially about numerical calculation by using AMD. They also appreciate the encouragement by Professor Y.Abe.

## REFERENCES

- 1) Y.Fujiwara, H.Horiuchi, K.Ikeda, M.Kamimura, K.Katō, Y.Suzuki, and E.Uegaki, *Prog. Theor. Phys. Suppl.* **68** (1980), 60.
- 2) Y.Fukushima and Kamimura, *Proc. Int. Conf. on Nuclear Structure, Tokyo, 1977*, 225.
- 3) E.Uegaki, S.Okabe, Y.Abe and H.Tanaka, *Prog. Theor. Phys.* **57** (1977), 1262.  
E.Uegaki, Y.Abe, S.Okabe and H.Tanaka,  
*Prog. Theor. Phys.* **59** (1978), 1031; **62** (1979), 1621.
- 4) H.Horiuchi, *Prog. Theor. Phys.* **51** (1974), 1266; **53** (1975), 447.
- 5) S.Cohen and D.Kurath, *Nucl. Phys.* **73** (1965), 1.
- 6) L.Buchmann *et al.* *Phys. Rev. Lett.* **70** (1993), 726.
- 7) Z.Zhao, R.H.France III, K.S.Lai, S.L.Rugari and M.Gai  
*Phys. Rev. Lett.* **70** (1993), 2066.
- 8) H.Horiuchi, *Proc.INS-IPCR Int.Symp.on Cluster Structure of Nuclei  
and Transfer Reaction Induced by Heavy-Ions, Tokyo, 1975*, 41.
- 9) Y.Suzuki, *Prog. Theor. Phys.* **56** (1976), 111.
- 10) Y.Suzuki, T.Ando and B.Imanishi, *Nucl. Phys.* **A 295** (1978), 365.
- 11) F.Nemoto and H.Bandō, *Prog. Theor. Phys.* **47** (1972), 1210.  
T.Matsuse and M.Kamimura, *Prog. Theor. Phys.* **49** (1973), 1765.  
T.Matsuse, M.Kamimura and Y.Fukushima, *Prog. Theor. Phys.* **53** (1975), 706.
- 12) Y.Fujiwara, H.Horiuchi and R.Tamagaki, *Prog. Theor. Phys.* **61** (1979), 1629.  
Y.Fujiwara, *Prog. Theor. Phys.* **62** (1979), 122,138.  
H.Horiuchi, *Proceedings of the International Symposium on Nuclear Collisions and  
Their Microscopic Description, Bled, 1977*, 251.
- 13) K.Katō and H.Bandō,  
*Prog. Theor. Phys.* **54** (1975), 1887; **62** (1979), 644.
- 14) K.Ikeda, N.Takigawa and H.Horiuchi, *Prog. Theor. Phys. Suppl. Extra Number* (1968),  
464;
- 15) Wuosmma *et al.*, *Phys. Rev. Lett.* **68** (1992), 1295.
- 16) W.D.M.Rea, A.C.Merchant and B.Buck, *Phys.Rev.Lett* **69** (1992), 3709.
- 17) A.Ono, H.Horiuchi, T.Maruyama and A.Ohnishi,  
*Prog.Theor.Phys.* **87** (1992), 1185; *Phys.Rev.Lett.* **68** (1992), 2898.
- 18) H.Horiuchi, M.Maruyama, A.Ohnishi and S.Yamaguchi, Preprint KUNS 1028.
- 19) Y.Kanada-En'yo and H.Horiuchi, *Prog. Theor. Phys.* **93** (1995), 115.
- 20) Y.Kanada-En'yo, H.Horiuchi and A.Ono, Preprint KUNS 1320.
- 21) Y.Kanada-En'yo and H.Horiuchi Preprint KUNS 1329.
- 22) D.Brink,*Proc. Int. School of Phys.- < ENRICO FERMI >*, course 36, 247.
- 23) Y.Fukatsu and K.Katō, *Prog. Theor. Phys.* **87** (1992), 151.
- 24) A.Tohsaki, *Phys. Rev.* **C49** (1994), 1814.
- 25) A.B.Volkov *Nucl. Phys.* **74** (1965) 33,
- 26) T.H.R.Skyrme, *Nucl. Phys.* **9** (1959), 615.
- 27) D.M.Brink and E.Boeker, *Nucl. Phys.* **A91** (1967), 1.
- 28) J.Zhang, W.D.M.Rea and A.C. Merchant, *Nucl. Phys.* **A575** (1994), 61.
- 29) P.Descouvemont, *Phys. Rev.* **C47** (1992), 210.

- 30) P.Descouvemont and D.Baye, Nucl. Phys. **A487** (1988), 420; **A567** (1994), 341; **A573** (1994), 28.
- 31) T.Yamada, K.Ikeda, T.Motoba and H.Bandō , Phys. Rev. **C38**(1988), 854.

## TABLES

Table I: Effective Interactions used here; a) potential forms and b) parameters of the Tohsaki No.1 force.

a)					
Volkov force	$V(r) = (W - MP^\sigma P^\tau)$ $\times (-60 \exp(-r^2/1.80^2) + 60 \exp(-r^2/1.01^2)) \quad (\text{MeV})$ where, $W = 1 - M$				
Volkov No.2 force	$V(r) = (W - MP^\sigma P^\tau)$ $\times (-60.65 \exp(-r^2/1.80^2) + 60.14 \exp(-r^2/1.01^2)) \quad (\text{MeV})$				
Tohsaki No.1 force	$V_{ij}^{(2)} = \sum_n (W_n^{(2)} - M_n^{(2)} P_{ij}^\sigma P_{ij}^\tau) v_n^{(2)} \exp(-r_{ij}^2/r_n^2) \quad (\text{MeV})$ $V_{ij}^{(3)} = \sum_n (W_n^{(3)} - M_n^{(3)} P_{ij}^\sigma P_{ij}^\tau) \times (W_n^{(3)} - M_n^{(3)} P_{jk}^\sigma P_{jk}^\tau)$ $\times v_n^{(3)} \exp(-r_{ij}^2/r_n^2 - r_{jk}^2/r_n^2) \quad (\text{MeV})$ where, $W^{(2)} = 1 - M^{(2)}$ and $W^{(3)} = 1 - M^{(3)}$				
b)					
n	$r_n$ (fm)	$v_n^{(2)}$ (MeV)	$M_n^{(2)}$	$v_n^{(3)}$ (MeV)	$M_n^{(3)}$
1	2.5	-5.00	0.750	-0.31	0.0
2	1.8	-43.51	0.462	7.73	0.0
3	0.7	60.38	0.522	219.00	1.909

Table II: GCM basis sets for  $^{12}\text{C}$ , which are specified by constraint values of the principal quantum numbers  $n_x$ ,  $n_y$ , and  $n_z$ .

	set I			set II				set I			set II		
	$n_x$	$n_y$	$n_z$	$n_x$	$n_y$	$n_z$		$n_x$	$n_y$	$n_z$	$n_x$	$n_y$	$n_z$
1	0.0	2.0	12.0	0.0	4.1	4.1	16	0.0	7.0	7.0	0.0	4.0	9.0
2	0.0	2.0	16.0	0.0	3.0	6.0	17	0.0	7.0	11.0	0.0	5.0	8.0
3	0.0	3.0	10.0	0.0	2.0	8.0	18	0.0	7.0	15.0	0.0	0.0	14.0
4	0.0	3.0	14.0	0.0	4.0	6.0	19	0.0	7.0	19.0	0.0	1.0	13.0
5	0.0	3.0	18.0	0.0	1.0	10.0	20	0.0	9.0	9.0	0.0	2.0	12.0
6	0.0	4.0	4.5	0.0	3.0	8.0	21	0.0	9.0	13.0	0.0	3.0	11.0
7	0.0	4.0	8.0	0.0	4.0	7.0	22	0.0	9.0	17.0	0.0	4.0	10.0
8	0.0	4.0	12.0	0.0	0.0	12.0	23	0.0	9.0	21.0	0.0	6.0	8.0
9	0.0	4.0	16.0	0.0	2.0	10.0	24	0.0	11.0	11.0	0.0	0.0	15.0
10	0.0	4.0	20.0	0.0	3.0	9.0	25	0.0	11.0	15.0	0.0	1.0	14.0
11	0.0	5.0	5.0	0.0	4.0	8.0	26	0.0	11.0	19.0	0.0	2.0	13.0
12	0.0	5.0	9.0	0.0	6.0	6.0	27	0.0	13.0	13.0	0.0	3.0	12.0
13	0.0	5.0	13.0	0.0	1.0	12.0	28	0.0	13.0	17.0	0.0	4.0	11.0
14	0.0	5.0	17.0	0.0	2.0	11.0	29	0.0	13.0	21.0	0.0	5.0	10.0
15	0.0	5.0	21.0	0.0	3.0	10.0	30	0.0	15.0	15.0	0.0	6.0	9.0

Table III: GCM basis sets for  $^{16}\text{C}$ , which are specified by constraint values of the principal quantum numbers  $n_x$ ,  $n_y$ , and  $n_z$ .

	$n_x$	$n_y$	$n_z$		$n_x$	$n_y$	$n_z$		$n_x$	$n_y$	$n_z$
1	4.5	4.0	4.0	11	8.0	5.0	5.0	21	4.0	8.0	8.0
2	5.0	4.0	4.0	12	12.0	5.0	5.0	22	6.0	8.0	8.0
3	6.0	4.0	4.0	13	16.0	5.0	5.0	23	8.0	8.0	8.0
4	7.0	4.0	4.0	14	20.0	5.0	5.0	24	12.0	8.0	8.0
5	8.0	4.0	4.0	15	4.0	6.0	6.0	25	16.0	8.0	8.0
6	12.0	4.0	4.0	16	6.0	6.0	6.0	26	20.0	8.0	8.0
7	16.0	4.0	4.0	17	8.0	6.0	6.0	27	4.0	10.0	10.0
8	20.0	4.0	4.0	18	12.0	6.0	6.0	28	8.0	10.0	10.0
9	4.0	5.0	5.0	19	16.0	6.0	6.0	29	12.0	10.0	10.0
10	6.0	5.0	5.0	20	20.0	6.0	6.0	30	16.0	10.0	10.0

Table IV: The size parameter  $\nu$  and the numbers of the basis states used in GCM calculation for each interaction.

Forces	$\nu$ (fm $^{-2}$ )	Base No. ( $^{12}\text{C}$ )	Base No. ( $^{16}\text{O}$ )
Skyrme II	0.18	25	20
Tohsaki No.1	0.23	25	20
BB No.1	0.23	25	20

Table V: Energies calculated by GCM with various effective interactions.

	$^{12}\text{C}$	$\alpha$	$^{16}\text{O}$ $0_1^+$	$^{16}\text{O}$ $0_2^+$	$^{12}\text{C}+\alpha$	$^{12}\text{C}+\alpha$ - $^{16}\text{O}$
Volkov2 $M = 0.63$	-82.0	-27.4	-127.6	-109.2	-109.4	18.2
Skyrme II	-76.4	-25.2	-123.0	-101.6	-101.6	21.4
Tohsaki No.1	-86.4	-27.3	-130.5	-113.5	-113.7	16.8
B-B No.1	-76.5	-27.0	-107.8	-95.1	-103.5	4.3
experiment	-92.2	-28.3	-127.6	-121.5	-120.5	7.2

Table VI: Comparison of the GCM calculation with the  $SU_3$  limit calculation in Ref.<sup>24</sup>

		Tohsaki $SU_3$	GCM	experiment
$^{12}\text{C}$	Ground st. energy (MeV)	-75.2	-86.4	-92.2
	Size parameter $\nu$ (fm $^{-2}$ )	0.18	0.23	
$^{16}\text{O}$	Ground st. energy (MeV)	-123.0	-130.5	-127.6
	Size parameter (fm $^{-2}$ )	0.175	0.23	

Energy Surface of  $^{12}\text{C}$  (unprojected)

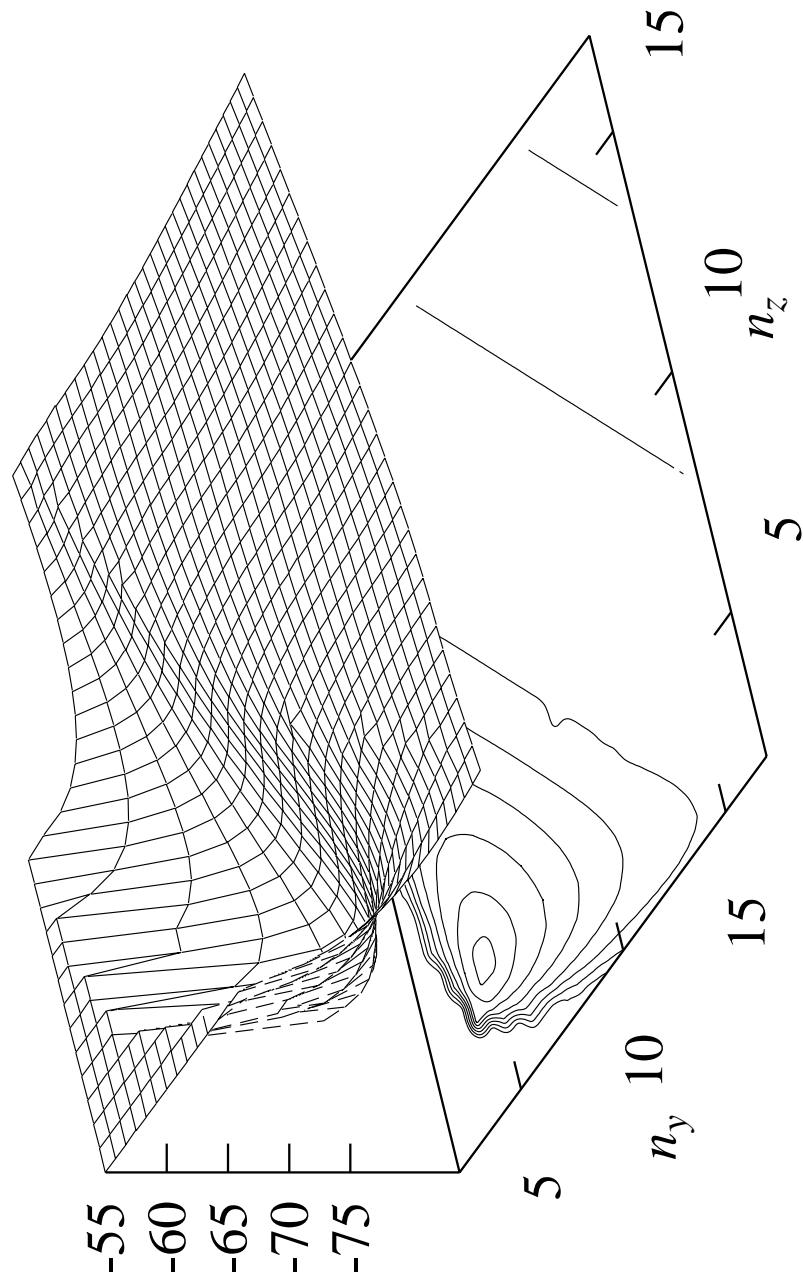


Figure 1: Energy surface and contour lines of  $^{12}\text{C}$  before  $J^\pi$ -projection. See the text for detail.

Energy Surface of  $^{12}\text{C}$  (projected to  $0^+$ )

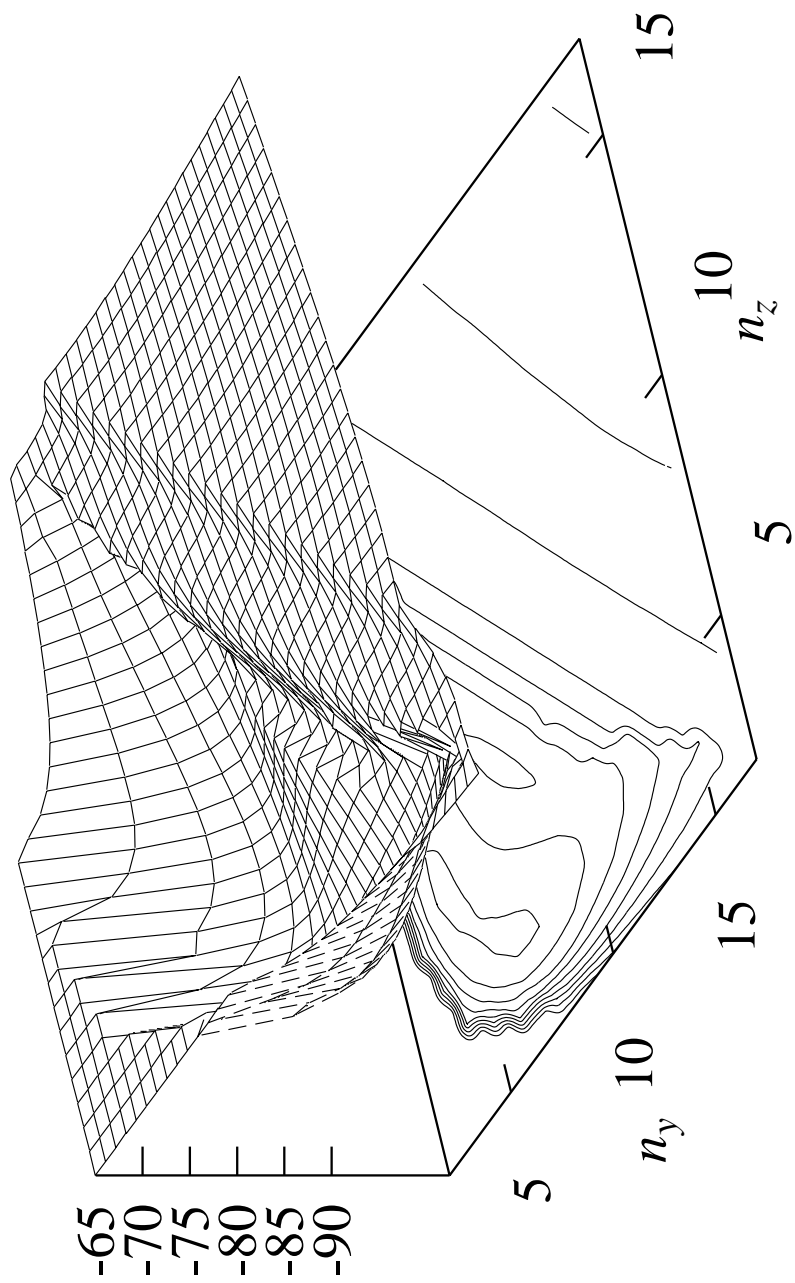


Figure 2: Energy Surface and contour lines of  $^{12}\text{C}$  after projection to  $0^+$ . See the text for detail.

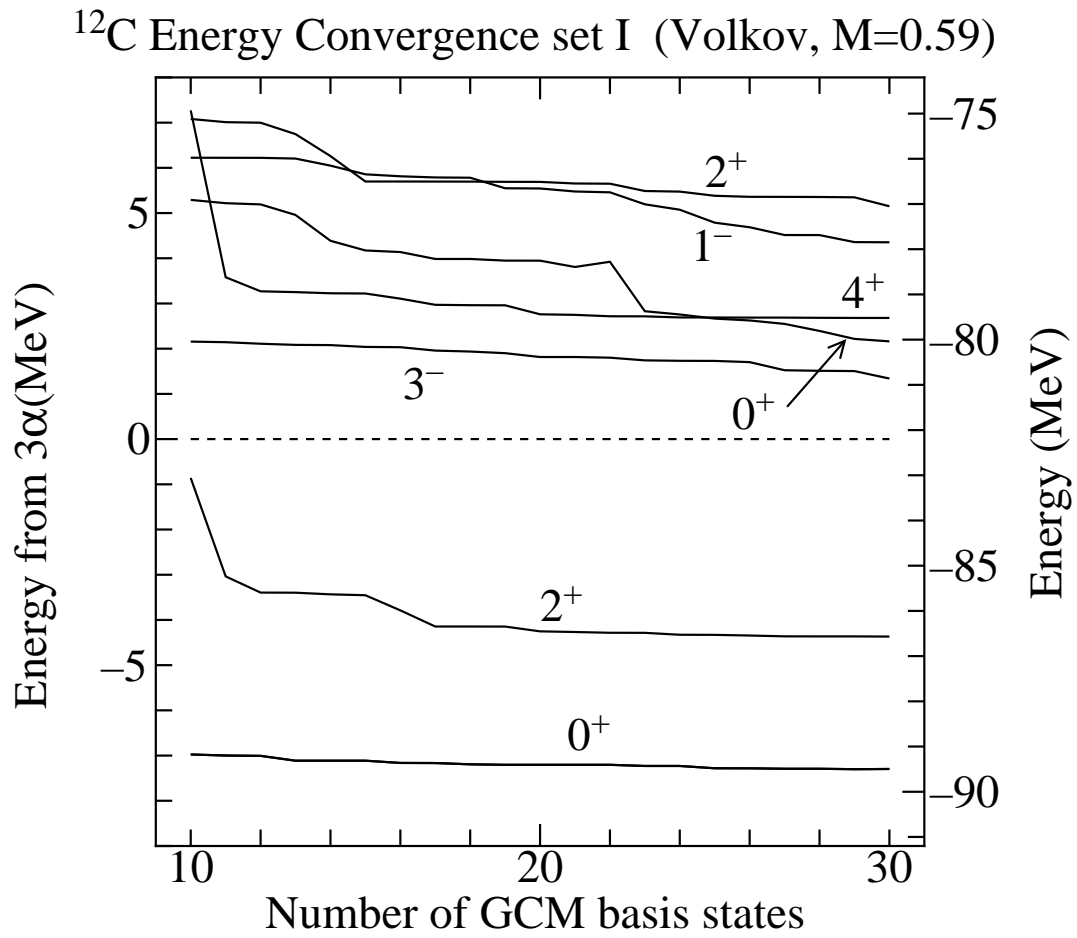


Figure 3: Energy convergence of levels of  $^{12}\text{C}$  with GCM basis set I. The GCM basis states are arranged in order of the small diagonal matrix elements of the Hamiltonian.

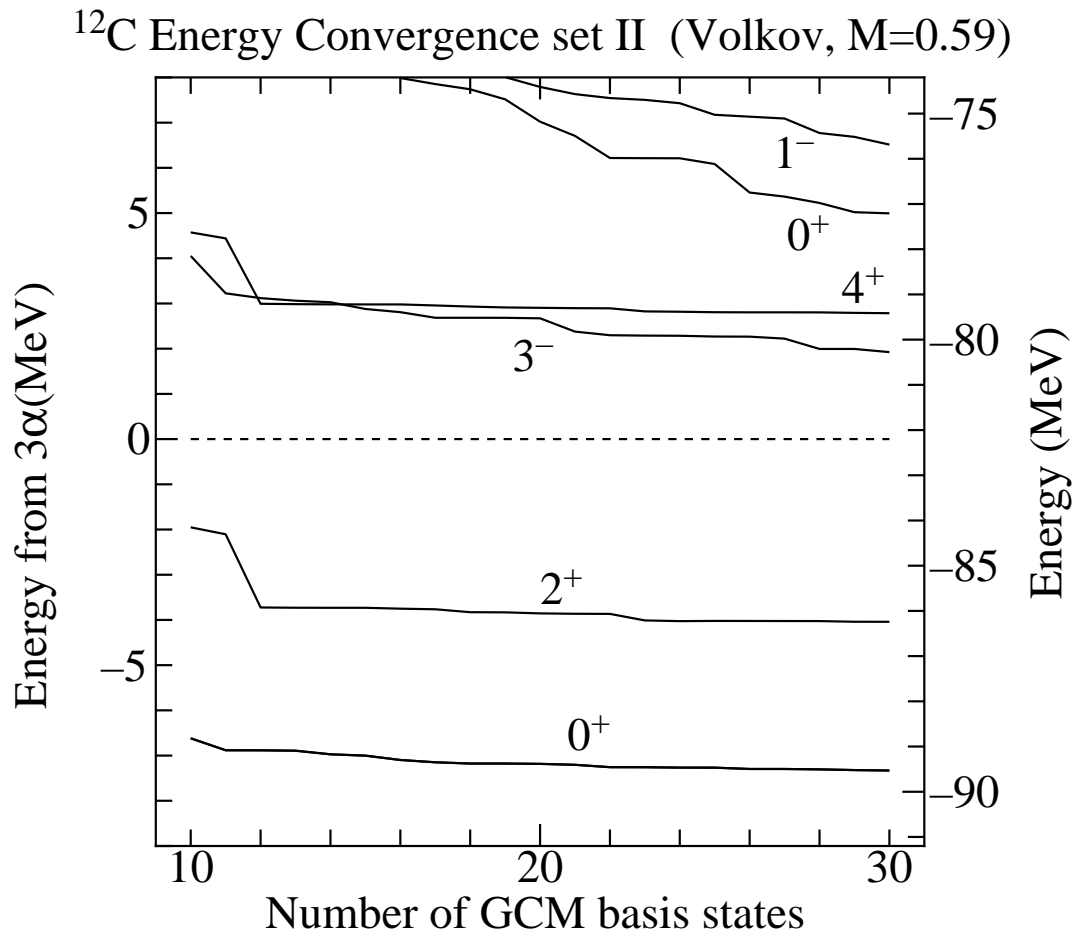


Figure 4: Energy convergence of levels of  $^{12}\text{C}$  with GCM basis set II. The GCM basis states are arranged in order of the small diagonal matrix elements of the Hamiltonian.

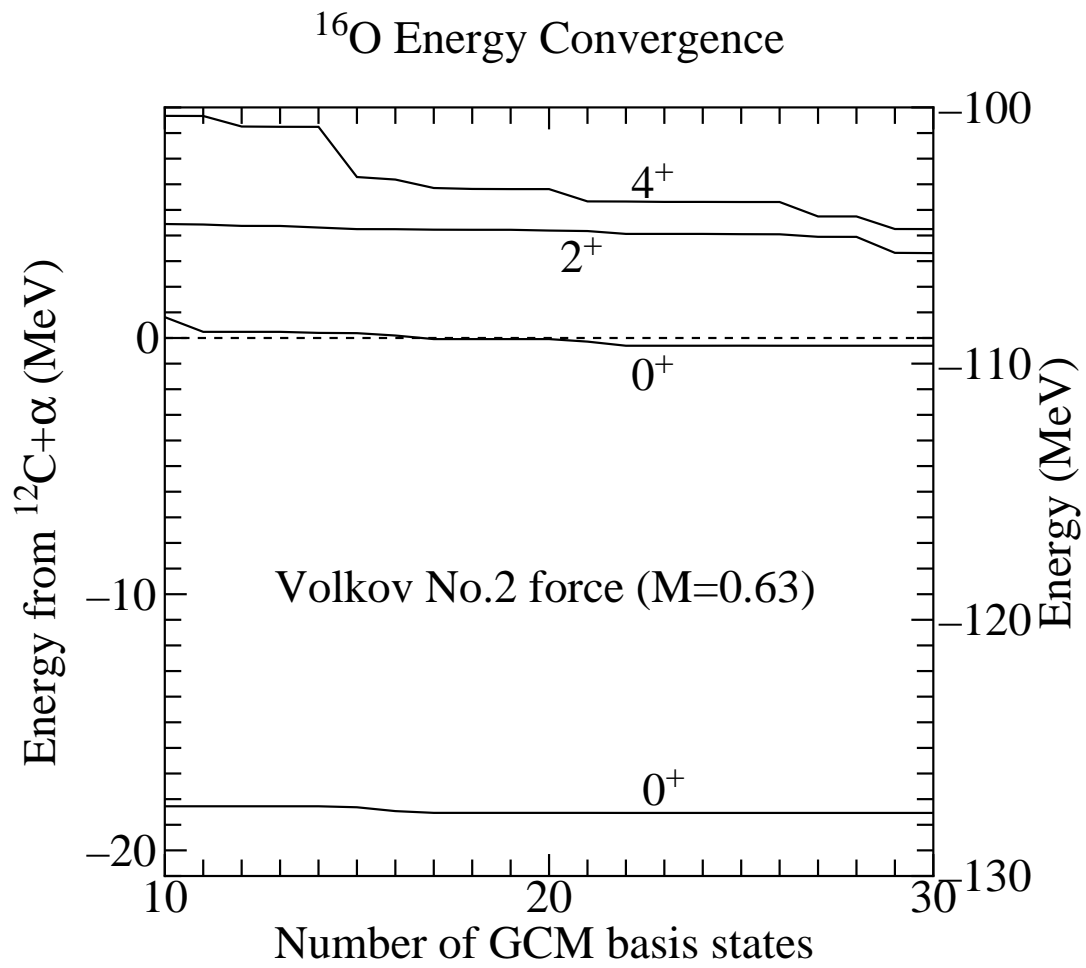


Figure 5: Energy convergence of levels of  $^{16}\text{O}$ . The GCM basis states are arranged in order of the small diagonal matrix elements of the Hamiltonian.

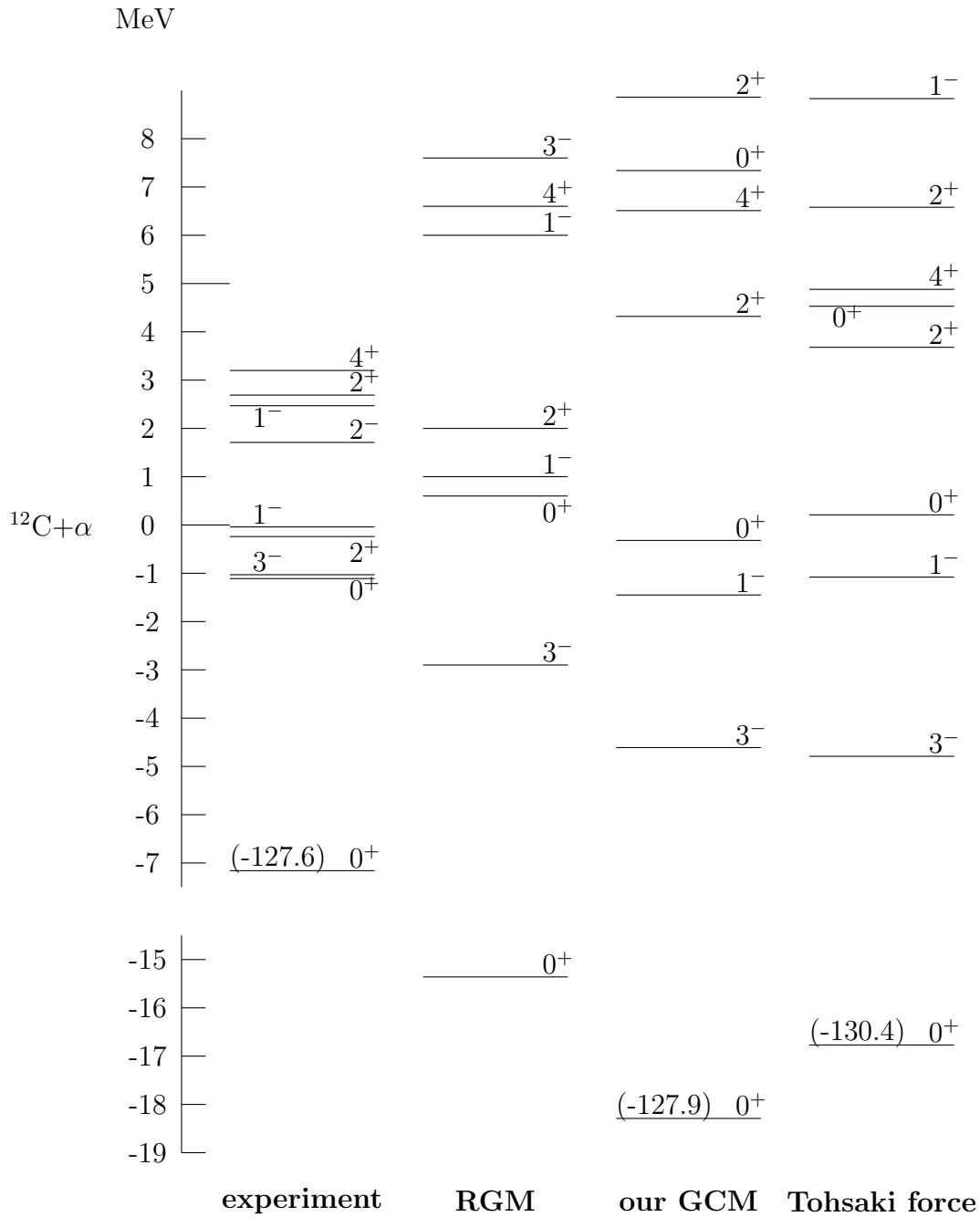


Figure 6: Energy levels of  $^{16}\text{O}$

All energies are measured from the  $^{12}\text{C}+\alpha$  threshold(dashed line). The values in a parenthesis above the ground state present the total energies. The result of RGM is taken from Ref.<sup>8)</sup>, where the Volkov No.2 with  $M=0.67$ . The present GCM results are presented for the Volkov No.2 force with  $M=0.63$  (Volkov No.2), and for the Tohsaki No.1 force (Tohsaki No.1). The size parameter  $\nu=0.23 \text{ fm}^{-2}$  is used in the present GCM calculation.

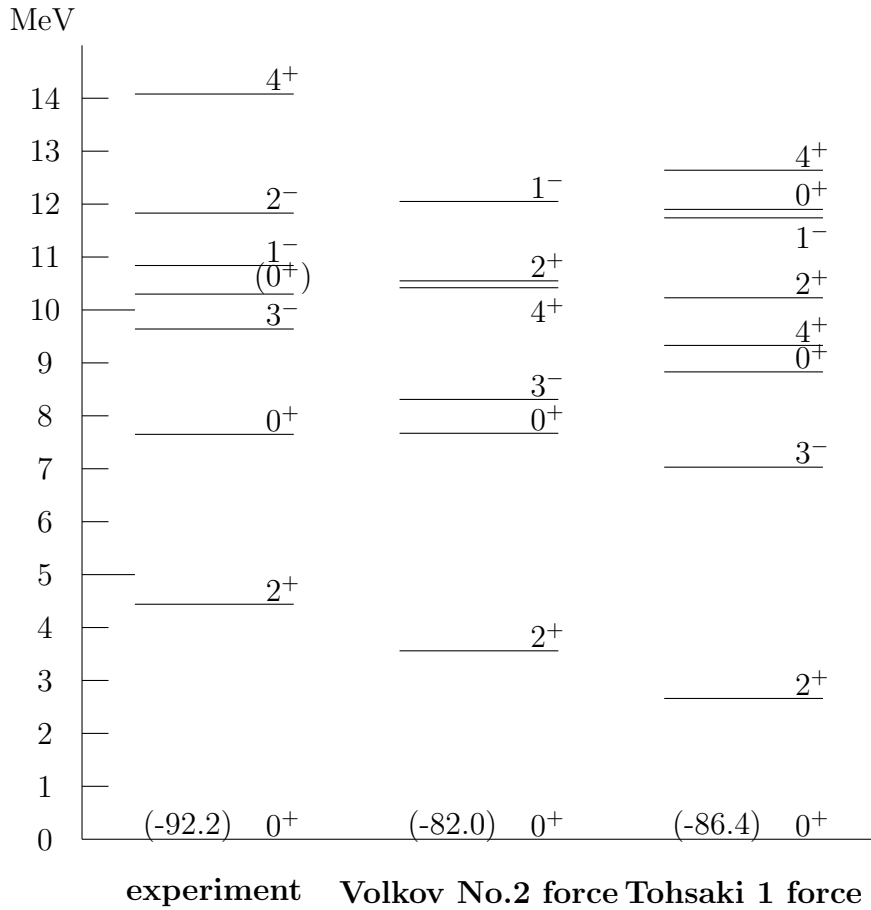


Figure 7: Energy levels of  $^{12}\text{C}$ . The values in a parenthesis above the ground state present the total energies. The present GCM results are presented for the Volkov No.2 force with  $M=0.63$  (Volkov No.2), and for the Tohsaki No.1 force (Tohsaki No.1). The size parameter  $\nu=0.23 \text{ fm}^{-2}$  is used in the present GCM calculation.